Available online at www.sciencedirect.com
SCIENCE DIRECT®
Journal of Power Sources 119–121 (2003) 644–648
JOURNAL OF POWER SOURCES
www.elsevier.com/locate/jpowsour

Crystal and electronic structures of superstructural $Li_{1-x}[Co_{1/3}Ni_{1/3}Mn_{1/3}]O_2$ $(0 \leq x \leq 1)$

Yukinori Koyama[a], Isao Tanaka[a], Hirohiko Adachi[a], Yoshinari Makimura[b], Tsutomu Ohzuku[b,*]

[a]*Department of Materials Science and Engineering, Kyoto University, Yoshida Hon-machi, Sakyo, Kyoto 606-8501, Japan*
[b]*Department of Applied Chemistry, Graduate School of Engineering, Osaka City University (OCU), Sugimoto 3-3-138, Sumiyoshi, Osaka 558-8585, Japan*

Abstract

Crystal and electronic structures of two model crystals for $Li[Co_{1/3}Ni_{1/3}Mn_{1/3}]O_2$ have been investigated using first principles calculations. One is so-called superlattice model of $[\sqrt{3} \times \sqrt{3}]R30^\circ$-type in triangular lattice of sites and the other is piled-up model among CoO_2, NiO_2 and MnO_2 slabs. For both models, the formal charges of Co, Ni and Mn are, respectively, estimated to be +3, +2 and +4 from the interatomic distances and electronic structures. The formation energy for a superlattice model is −0.17 eV while that for a piled-up model is +0.06 eV, indicating that $Li[Co_{1/3}Ni_{1/3}Mn_{1/3}]O_2$ having a $[\sqrt{3} \times \sqrt{3}]R30^\circ$-type superlattice can be prepared when the processing method is exploited. The solid-state redox reactions in a superlattice model are also calculated and predicted that the reaction in the ranges of $0 \leq x \leq 1/3$, $1/3 \leq x \leq 2/3$ and $2/3 \leq x \leq 1$ in $Li_{1-x}[Co_{1/3}Ni_{1/3}Mn_{1/3}]O_2$ consists of Ni^{2+}/Ni^{3+}, Ni^{3+}/Ni^{4+} and Co^{3+}/Co^{4+}, respectively, with smaller change in unit-cell volume associated with lithium insertion reaction than those of $LiCoO_2$, $LiNiO_2$ and $LiMnO_2$.

Keywords: Crystal structure; Electronic structure; $Li_{1-x}[Co_{1/3}Ni_{1/3}Mn_{1/3}]O_2$ $(0 \leq x \leq 1)$

1. Introduction

A number of studies on lithium transition-metal oxides have been performed for electrode materials of lithium-ion batteries. Among them, layered $LiMeO_2$ (Me = 3d transition-metal element) with an α-$NaFeO_2$-structural type have been widely investigated (see for an example a review article [1]). The crystal structure of the α-$NaFeO_2$-type is of an ordered rock-salt type such that Li and Me ions occupy alternate (1 1 1) layers. Among the layered oxides, $LiCoO_2$ was the first material that was investigated and implemented as a positive electrode for lithium-ion batteries, and the lithium-ion batteries with $LiCoO_2$ and graphite have been developed at a quite high level. The cell performance, however, approaches a critical level for many reasons unless material innovation has been done.

In the present study, we directed our attention to a new layered oxide of $Li[Co_{1/3}Ni_{1/3}Mn_{1/3}]O_2$ [2]. In this compound, Co, Ni and Mn may be put into lattice positions to form $[\sqrt{3} \times \sqrt{3}]R30^\circ$-type superlattice of the α-$NaFeO_2$-type by a simple geometrical inspection. If it comes true, this material may be expected to show new functions due to the superlattice structure. We investigate its crystal and electronic structures using first principles calculations. A possible solid-state redox reaction associated with lithium insertion and extraction is discussed.

2. Computational procedure

We employed two structural models shown in Fig. 1 for $Li[Co_{1/3}Ni_{1/3}Mn_{1/3}]O_2$. The first model illustrated in Fig. 1a consists of $[Co_{1/3}Ni_{1/3}Mn_{1/3}]O_2$ slabs of the $[\sqrt{3} \times \sqrt{3}]R30^\circ$-type superlattice in Wood's notation based on basal net in triangular lattice of sites. This structural model is called superlattice model hereafter. The way to stack the slabs is not unique. Therefore, we employed one of the ways having the space-group symmetry of $P3_112$. The second model illustrated in Fig. 1b consists of CoO_2, NiO_2 and MnO_2 slabs piled up regularly, called piled-up model hereafter. The two models were thus selected as extreme cases in terms of the distribution of Co, Ni and Mn to form $Li[Co_{1/3}Ni_{1/3}Mn_{1/3}]O_2$.

Total energies and electronic structures were calculated by the plane-wave pseudopotential method [3]. Ultrasoft

* Corresponding author. Fax: +81-6-66052693.
E-mail address: ohzuku@a-chem.eng.osaka-cu.ac.jp (T. Ohzuku).

0378-7753/03/$ – see front matter © 2003 Elsevier Science B.V. All rights reserved.
doi:10.1016/S0378-7753(03)00194-0

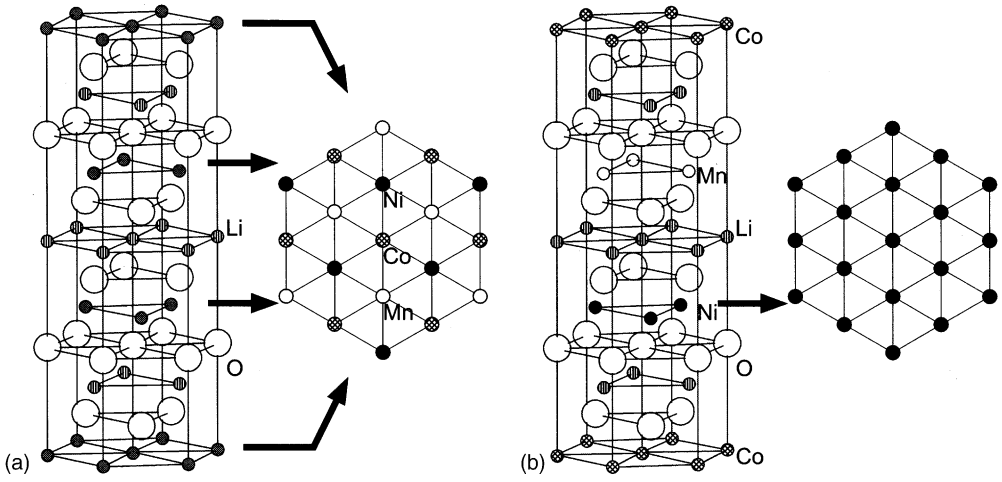

Fig. 1. Structural models for superstructural $Li[Co_{1/3}Ni_{1/3}Mn_{1/3}]O_2$: (a) consists of $[Co_{1/3}Ni_{1/3}Mn_{1/3}]O_2$ slabs with the superlattice of $[\sqrt{3}\times\sqrt{3}]R30^\circ$; and (b) consists of alternate CoO_2, NiO_2 and MnO_2 slabs. Li, Co, Ni, Mn and O ions are denoted by striped-patterned, crossed-patterned, filled, small open and large open circles, respectively.

pseudopotentials [4] were used with a plane-wave cutoff of 500 eV. The local spin density approximation (LSDA) [5] was applied with ferromagnetic spin ordering. Reciprocal space sampling for integration was done with 7 points for the superlattice model and with 15 points for the piled-up model in the irreducible Brillouin zone. Number of sampling points was so determined that the density of points in the reciprocal space was almost the same. All lattice parameters and internal atomic positions were optimized. For comparison, total energy and electronic structure calculations of $LiCoO_2$, $LiNiO_2$ and $LiMnO_2$ were also performed with the same scheme for $Li[Co_{1/3}Ni_{1/3}Mn_{1/3}]O_2$. Actually, $LiMnO_2$ with the layered structure is distorted because of Jahn-Teller Mn^{3+} ion. The regular α-$NaFeO_2$-type structure was, however, used for simple comparison. Since Mishra and Ceder reported [6] that the application of the LSDA to the layered $LiMnO_2$ led to a wrong spin-state of low-spin Mn^{3+}, we fixed the spin moment of $LiMnO_2$ to show high-spin Mn^{3+}.

3. Results and discussion

3.1. Crystal and electronic structures of $Li[Co_{1/3}Ni_{1/3}Mn_{1/3}]O_2$

Calculated lattice parameters, a and c in the original α-$NaFeO_2$-type, for both models on $Li[Co_{1/3}Ni_{1/3}Mn_{1/3}]O_2$ are listed in Table 1, together with those of $LiCoO_2$, $LiNiO_2$ and $LiMnO_2$ and some experimental results available in literatures [2,7]. Although several calculations of $LiCoO_2$ using the LSDA were already reported [8,9], there are some differences in their lattice parameters. Our result is very similar to that by Wolverton and Zunger [9] using the full potential, all-electron linearized augmented plane-wave method. Our results tend to underestimate lattice constants, especially parameter of c as were already reported [8,9]. Comparison of lattice parameters and interatomic distances will be done only among our results. Average interatomic distances between transition-metal and oxygen ions in the four compounds are listed in Table 2. The distances of Co–O in both models for $Li[Co_{1/3}Ni_{1/3}Mn_{1/3}]O_2$ are almost the same as that in $LiCoO_2$. The distances of Ni–O in $Li[Co_{1/3}Ni_{1/3}Mn_{1/3}]O_2$ are longer than that in $LiNiO_2$. Conversely, the distances of Mn–O in $Li[Co_{1/3}Ni_{1/3}Mn_{1/3}]O_2$ are rather shorter than that in $LiMnO_2$. These results suggest that the local electronic structure of Co in $Li[Co_{1/3}Ni_{1/3}Mn_{1/3}]O_2$ is almost the same as that in $LiCoO_2$ while those of Ni and Mn in $Li[Co_{1/3}Ni_{1/3}Mn_{1/3}]O_2$ and, respectively, different from those in $LiNiO_2$ and $LiMnO_2$.

Densities of states (DOS) of both models on $Li[Co_{1/3}Ni_{1/3}Mn_{1/3}]O_2$ are shown in Fig. 2. Since the transition-metal ions occupy the octahedral sites in the sublattice of oxygen, 3d bands of transition-metal elements are split into the t_{2g}-like and e_g-like bands. In the figure, O-2p and Me-t_{2g}

Table 1
Lattice parameters, a and c in an α-$NaFeO_2$-structural type, of both models for $Li[Co_{1/3}Ni_{1/3}Mn_{1/3}]O_2$ as shown in Fig. 1 and of $LiCoO_2$, $LiNiO_2$ and $LiMnO_2$ with a regular α-$NaFeO_2$-type

Compound	Lattice parameters	
	a (Å)	c (Å)
$Li[Co_{1/3}Ni_{1/3}Mn_{1/3}]O_2$		
Calculated (Fig. 1a)	2.831	13.88
Calculated (Fig. 1b)	2.827	13.94
Experimental [2]	2.867	14.246
$LiCoO_2$		
Calculated	2.813	13.59
Experimental [7]	2.814	14.044
$LiNiO_2$		
Calculated	2.837	13.71
Experimental [7]	2.880	14.187
$LiMnO_2$		
Calculated	2.932	14.16

Table 2
Average interatomic distances between transition-metal and oxygen in both models for $Li[Co_{1/3}Ni_{1/3}Mn_{1/3}]O_2$ as shown in Fig. 1 and in $LiCoO_2$, $LiNiO_2$ and $LiMnO_2$ with a regular α-$NaFeO_2$-type

Compound	Average interatomic distance (Å)		
	Co–O	Ni–O	Mn–O
$Li[Co_{1/3}Ni_{1/3}Mn_{1/3}]O_2$ (Fig. 1a)	1.92	2.02	1.94
$Li[Co_{1/3}Ni_{1/3}Mn_{1/3}]O_2$ (Fig. 1b)	1.92	1.99	1.96
$LiCoO_2$	1.91	–	–
$LiNiO_2$	–	1.94	–
$LiMnO_2$	–	–	2.03

and Me-e_g (Me = Co, Ni and Mn) bands are marked with respect to the local DOS. For the superlattice model illustrated in Fig. 1a, Co-t_{2g}, Ni-t_{2g}, Mn-t_{2g} and Ni-e_g bands with up-spin state and Co-t_{2g} and Ni-t_{2g} bands with down-spin state are fully occupied, while Mn-e_g band with up-spin state is empty. These results indicate that the formal charges of Co, Ni and Mn in $Li[Co_{1/3}Ni_{1/3}Mn_{1/3}]O_2$ are +3, +2 and +4, respectively. For the piled-up model illustrated in Fig. 1b, the bands in the DOS are similar to those for superlattice model, but they are mixed up to show broad peaks. Consequently, the electronic description in term of the formal charge is the same for the both models, which is consistent with the results on the interatomic distances between transition-metal and oxygen ions as described above.

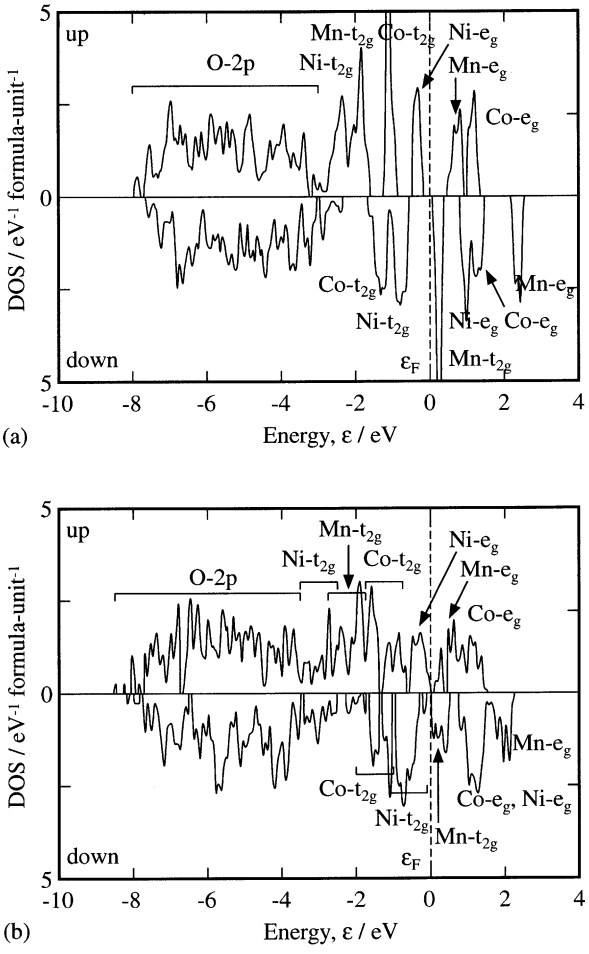

Fig. 2. Density of states of both models for $Li[Co_{1/3}Ni_{1/3}Mn_{1/3}]O_2$ as shown in Fig. 1. They are aligned so as to make the Fermi energy to be zero.

In order to estimate which of the two structures is most stable in advance, the formation energy of $Li[Co_{1/3}Ni_{1/3}Mn_{1/3}]O_2$ is calculated. In the present study, the formation energy of $Li[Co_{1/3}Ni_{1/3}Mn_{1/3}]O_2$ is defined as

$$\Delta E = E_{tot}[Li[Co_{1/3}Ni_{1/3}Mn_{1/3}]O_2] - \tfrac{1}{3}\{E_{tot}[LiCoO_2] + E_{tot}[LiNiO_2] + E_{tot}[LiMnO_2]\}, \quad (1)$$

where $E_{tot}[LiMeO_2]$ is the total energy of $LiMeO_2$ per a formula unit. The formation energy of the superlattice model was calculated to be −0.17 eV per a formula unit, and that of the piled-up model was calculated to be +0.06 eV. This clearly indicates that $Li[Co_{1/3}Ni_{1/3}Mn_{1/3}]O_2$ having a superlattice structure can be prepared and the piled-up structure is hardly expected to be prepared.

3.2. Changes in crystal and electronic structures due to the solid-state redox reaction

We will discuss the solid-state redox reaction in $Li[Co_{1/3}Ni_{1/3}Mn_{1/3}]O_2$ having a superlattice structure illustrated in Fig. 1a hereafter. For this purpose, calculations of $Li_{1-x}[Co_{1/3}Ni_{1/3}Mn_{1/3}]O_2$ ($0 \le x \le 1$) were performed. To focus on the solid-state redox reaction of transition-metal ions, we considered Li compositions only of $x = 0$, 1/3, 2/3 and 1. We assumed that the layered structure including the location of Co, Ni and Mn ions did not change during the reaction and the ordering of Li and its vacancy was the same as that of transition-metal ions. Under these assumptions, there are three choices of the arrangement of Li and its vacancy in each of $\square_{1/3}Li_{2/3}[Co_{1/3}Ni_{1/3}Mn_{1/3}]O_2$ and $\square_{2/3}Li_{1/3}[Co_{1/3}Ni_{1/3}Mn_{1/3}]O_2$. Thus, three calculations for the three arrangements were performed and the most energetically preferable arrangement was employed at each of $\square_{1/3}Li_{2/3}[Co_{1/3}Ni_{1/3}Mn_{1/3}]O_2$ and $\square_{2/3}Li_{1/3}[Co_{1/3}Ni_{1/3}Mn_{1/3}]O_2$. The differences in total energy among the arrangements were less than 0.02 eV per a formula unit at both compositions.

As shown in Fig. 2a, the highest occupied band in $Li[Co_{1/3}Ni_{1/3}Mn_{1/3}]O_2$ is the Ni-e_g band with up-spin state. Therefore, an electron is removed from the Ni-e_g band by the extraction of Li, and the Ni-e_g band becomes empty in $\square_{2/3}Li_{1/3}[Co_{1/3}Ni_{1/3}Mn_{1/3}]O_2$. Formal notation of solid-state reaction in the range of $0 \le x \le 2/3$ in $Li_{1-x}[Co_{1/3}Ni_{1/3}Mn_{1/3}]O_2$ is Ni^{2+}/Ni^{3+} and Ni^{3+}/Ni^{4+}. In $Li[Co_{1/3}Ni_{1/3}Mn_{1/3}]O_2$, the second highest occupied band is the Ni-t_{2g} with down-spin state. However, the extraction of Li changes its electronic structure, resulting in the highest occupied band of Co-t_{2g} with up-spin state in $\square_{2/3}Li_{1/3}[Co_{1/3}Ni_{1/3}Mn_{1/3}]O_2$, as shown in Fig. 3. Thus, the formal

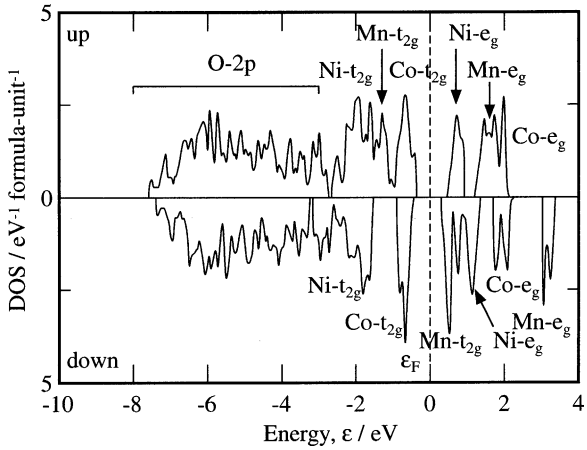

Fig. 3. Density of states of $\square_{2/3}Li_{1/3}[Co_{1/3}Ni_{1/3}Mn_{1/3}]O_2$ constituted of superstructural $[Co_{1/3}Ni_{1/3}Mn_{1/3}]O_2$ slabs.

redox reaction of Co^{3+}/Co^{4+} takes place in the range of $2/3 \leq x \leq 1$ in $Li_{1-x}[Co_{1/3}Ni_{1/3}Mn_{1/3}]O_2$.

Average voltage of $Li_{1-x}MeO_2$ in the range of $x_1 \leq x \leq x_2$ can be calculated by

$$V_{ave} = \frac{E_{tot}[Li_{1-x_2}MeO_2] - E_{tot}[Li_{1-x_1}MeO_2] + (x_2 - x_1)E_{tot}[Li]}{(x_2 - x_1)e}, \quad (2)$$

where $E_{tot}[\ ]$ is the total energy per a formula unit and e is the elementary electric charge. Calculated average voltages in the three ranges of $0 \leq x \leq 1/3$, $1/3 \leq x \leq 2/3$ and $2/3 \leq x \leq 1$ in $Li_{1-x}[Co_{1/3}Ni_{1/3}Mn_{1/3}]O_2$, $Li_{1-x}CoO_2$, $Li_{1-x}NiO_2$ and $Li_{1-x}MnO_2$ are summarized in Table 3. The calculated average voltage of $LiCoO_2$ in the present study in the whole range is 4.03 V and it is somewhat higher than reported values of 3.75 V [8] and 3.78 V [9]. Our result of $LiNiO_2$, which is 3.30 V, is also a little higher than the result by Aydinol et al. [8], which is 2.92 V. Perhaps, there is some inconsistency in the total energy of lithium metal, $E_{tot}[Li]$, in Eq. (2), although the same LSDA is used. Since the total energy of lithium metal affects only the absolute values of the voltage, not the relative values among the materials, the inconsistency does not give a significant problem in discussing voltages of lithium insertion electrodes. In the range of $0 \leq x \leq 1/3$ in $Li_{1-x}[Co_{1/3}Ni_{1/3}Mn_{1/3}]O_2$, the redox reaction is formally represented as Ni^{2+}/Ni^{3+}. Its voltage is, however, similar to that of $Li_{1-x}NiO_2$, where the redox reaction of Ni^{3+}/Ni^{4+} takes place. In the range of $1/3 \leq x \leq 2/3$, the formal redox reaction of Ni^{3+}/Ni^{4+} takes place both in $Li_{1-x}[Co_{1/3}Ni_{1/3}Mn_{1/3}]O_2$ and in $Li_{1-x}NiO_2$ and they show similar voltages. For more oxidation in $2/3 \leq x \leq 1$, $Li_{1-x}[Co_{1/3}Ni_{1/3}Mn_{1/3}]O_2$ shows a similar voltage to that of $Li_{1-x}CoO_2$, where the redox reaction of Co^{3+}/Co^{4+} takes place in each compound.

Table 3
Calculated average voltages of $Li[Co_{1/3}Ni_{1/3}Mn_{1/3}]O_2$ shown in Fig. 1a and of $LiCoO_2$, $LiNiO_2$ and $LiMnO_2$ with a regular α-$NaFeO_2$-type in the ranges of $0 \leq x \leq 1/3$, $1/3 \leq x \leq 2/3$ and $2/3 \leq x \leq 1$ in $Li_{1-x}MeO_2$

Compound	Average voltage (V)		
	$0 \leq x \leq 1/3$	$1/3 \leq x \leq 2/3$	$2/3 \leq x \leq 1$
$Li[Co_{1/3}Ni_{1/3}Mn_{1/3}]O_2$ (Fig. 1a)	2.99	3.30	4.50
$LiCoO_2$	3.51	4.02	4.55
$LiNiO_2$	2.94	3.35	3.61
$LiMnO_2$	2.46	2.90	3.11

Fig. 4 shows relative lattice parameters and unit-cell volume of $Li_{1-x}[Co_{1/3}Ni_{1/3}Mn_{1/3}]O_2$, $Li_{1-x}CoO_2$, $Li_{1-x}NiO_2$ and $Li_{1-x}MnO_2$ ($x = 0$, 1/3, 2/3 and 1). Values at $x = 0$ were used as standards. In the cases of $LiNiO_2$ and $LiMnO_2$, lattice parameter a decreases monotonically in all ranges. On the

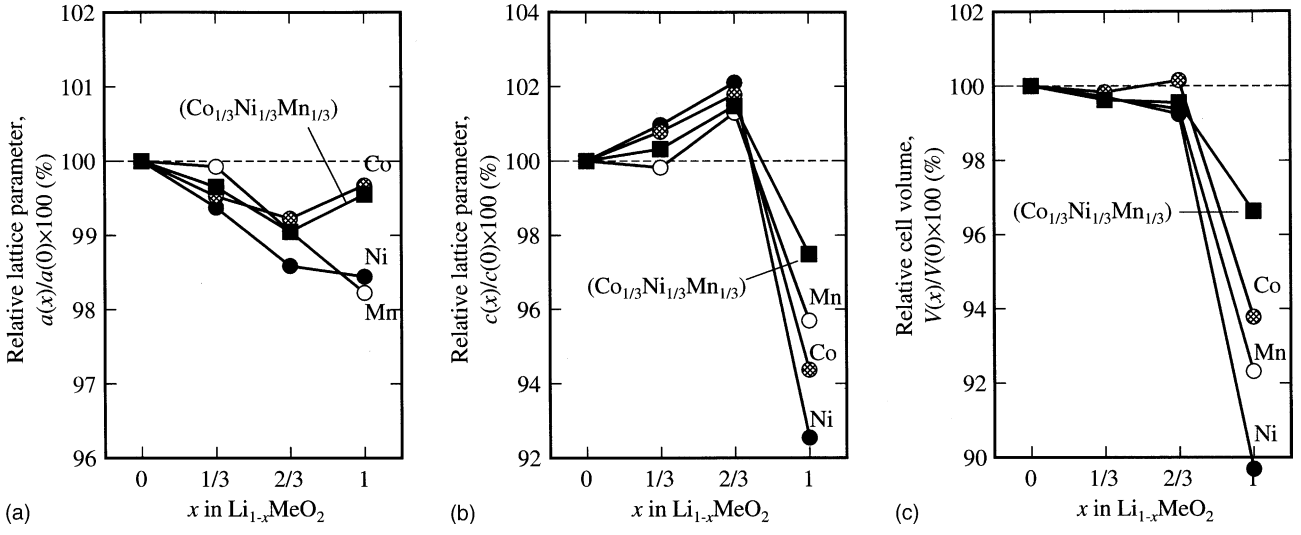

Fig. 4. Relative lattice parameters, a and c, and cell volume as function of x in $Li_{1-x}[Co_{1/3}Ni_{1/3}Mn_{1/3}]O_2$, $Li_{1-x}CoO_2$, $Li_{1-x}NiO_2$ and $Li_{1-x}MnO_2$. Values at $x = 0$ were used as standards. The data for $Li_{1-x}[Co_{1/3}Ni_{1/3}Mn_{1/3}]O_2$, $Li_{1-x}CoO_2$, $Li_{1-x}NiO_2$ and $Li_{1-x}MnO_2$ are denoted by filled square and crossed patterned, filled and open circles, respectively.

other hand, lattice parameter a of $Li[Co_{1/3}Ni_{1/3}Mn_{1/3}]O_2$ and $LiCoO_2$ decreases in the range of $0 \leq x \leq 2/3$. It then increases in the range of $2/3 \leq x \leq 1$. In the case of lattice parameter c, it increases slightly in the range of $0 \leq x \leq 2/3$ and it then decreases drastically afterwards in all compounds. Change in unit-cell volume in the range of $0 \leq x \leq 2/3$ is very small in all compounds, because of the opposite directions of changes in a and c. In the range of $2/3 \leq x \leq 1$, the change in the unit-cell volume corresponds to that in the lattice parameter of c. Therefore, a large decrease can be found in $LiCoO_2$, $LiNiO_2$ and $LiMnO_2$. Contrary to them, $Li[Co_{1/3}Ni_{1/3}Mn_{1/3}]O_2$ shows a small decrease. The small change in the unit-cell volume of $Li[Co_{1/3}Ni_{1/3}Mn_{1/3}]O_2$ may be beneficial to its electrochemical properties such as cycleability, shell life, or rate capability.

As were briefly discussed above, we have concluded that $Li[Co_{1/3}Ni_{1/3}Mn_{1/3}]O_2$ having a superlattice structure can be predicted by the first principles calculation, so that we believe that this material is materialized as a positive-electrode material for advanced lithium-ion batteries when the processing method to prepare such a material is exploited. Such an approach is still under way in our group while some of our trials have already been reported [2,10].

References

[1] R. Koksbang, J. Barker, H. Shi, M.Y. Saïdi, Solid State Ionics 84 (1996) 1.
[2] T. Ohzuku, Y. Makimura, Chem. Lett. (2001) 642.
[3] V. Milman, B. Winkler, J.A. White, C.J. Pickard, M.C. Payne, E.V. Akhmatskaya, R.H. Nobes, Int. J. Quant. Chem. 77 (2000) 895 (The CASTEP program code was used in the present study, Accelrys Inc., San Diego, CA).
[4] D. Vanderbilt, Phys. Rev. B 41 (1990) 7892.
[5] J.P. Perdew, A. Zunger, Phys. Rev. B 23 (1981) 5048.
[6] S.K. Mishra, G. Ceder, Phys. Rev. B 59 (1999) 6120.
[7] T. Ohzuku, A. Ueda, M. Nagayama, Y. Iwakoshi, H. Komori, Electrochim. Acta 38 (1993) 1159.
[8] M.K. Aydinol, A.F. Kohan, G. Ceder, K. Cho, J. Joannopoulos, Phys. Rev. B 56 (1997) 1354.
[9] C. Wolverton, A. Zunger, Phys. Rev. B 57 (1998) 2242.
[10] Y. Koyama, I. Tanaka, H. Adachi, Y. Makimura, N. Yabuuchi, T. Ohzuku, 2I18 and 2I19 in Abstract of the 42nd Battery Symposium in Japan, Yokohama, November 2001.